Video Article

Live Imaging Assay for Assessing the Roles of Ca^{2+} and Sphingomyelinase in the Repair of Pore-forming Toxin Wounds

Christina Tam[1], Andrew R. Flannery[1], Norma Andrews[1]

[1]Department of Cell Biology and Molecular Genetics, University of Maryland

Correspondence to: Christina Tam at cctam2002@yahoo.com

URL: https://www.jove.com/video/50531
DOI: doi:10.3791/50531

Keywords: Cellular Biology, Issue 78, Molecular Biology, Infection, Medicine, Immunology, Biomedical Engineering, Anatomy, Physiology, Biophysics, Genetics, Bacterial Toxins, Microscopy, Video, Endocytosis, Biology, Cell Biology, streptolysin O, plasma membrane repair, ceramide, endocytosis, Ca^{2+}, wounds

Date Published: 8/25/2013

Citation: Tam, C., Flannery, A.R., Andrews, N. Live Imaging Assay for Assessing the Roles of Ca^{2+} and Sphingomyelinase in the Repair of Pore-forming Toxin Wounds. *J. Vis. Exp.* (78), e50531, doi:10.3791/50531 (2013).

Abstract

Plasma membrane injury is a frequent event, and wounds have to be rapidly repaired to ensure cellular survival. Influx of Ca^{2+} is a key signaling event that triggers the repair of mechanical wounds on the plasma membrane within ~30 sec. Recent studies revealed that mammalian cells also reseal their plasma membrane after permeabilization with pore forming toxins in a Ca^{2+}-dependent process that involves exocytosis of the lysosomal enzyme acid sphingomyelinase followed by pore endocytosis. Here, we describe the methodology used to demonstrate that the resealing of cells permeabilized by the toxin streptolysin O is also rapid and dependent on Ca^{2+} influx. The assay design allows synchronization of the injury event and a precise kinetic measurement of the ability of cells to restore plasma membrane integrity by imaging and quantifying the extent by which the liphophilic dye FM1-43 reaches intracellular membranes. This live assay also allows a sensitive assessment of the ability of exogenously added soluble factors such as sphingomyelinase to inhibit FM1-43 influx, reflecting the ability of cells to repair their plasma membrane. This assay allowed us to show for the first time that sphingomyelinase acts downstream of Ca^{2+}-dependent exocytosis, since extracellular addition of the enzyme promotes resealing of cells permeabilized in the absence of Ca^{2+}.

Video Link

The video component of this article can be found at https://www.jove.com/video/50531/

Introduction

It has been known for several decades that plasma membrane repair after mechanical injury is a Ca^{2+}-dependent process[1,2]. Later studies showed that Ca^{2+} influx through the wound triggers a vigorous process of exocytosis of intracellular vesicles at the site of injury, which is required for resealing[3,4]. The rate of loss of a fluorescent dye loaded into the cytoplasm of cells was used to assess the speed of repair, and concluded that resealing was completed within <30 sec after injury[5]. Two models were initially proposed to explain the requirement for exocytosis in plasma membrane repair: 1) the "patch" model, which suggested that Ca^{2+} influx through the lesion triggers initially homotypic fusion of intracellular vesicles, forming a large "patch" that would then be applied to the plasma membrane to reseal the wound[6] and 2) the tension reduction model, which proposed that membrane added by Ca^{2+}-dependent exocytosis in the vicinity of the wound would reduce plasma membrane tension, facilitating resealing of the bilayer[7]. The role of Ca^{2+}-triggered exocytosis in plasma membrane repair was further reinforced by studies showing that lysosomes contain a Ca^{2+} sensor molecule, synaptotagmin VII, which facilitates their exocytosis and plasma membrane repair in injured cells[8,9,10,11].

However, additional evidence has indicated that exocytosis alone was not sufficient to promote plasma membrane repair. In addition to mechanical tears on the plasma membrane, a frequent form of cell injury is permeabilization by pore-forming toxins produced by bacteria[12,13] or immune cells[14,15]. Unlike mechanical tears, pore-forming proteins insert themselves on the plasma membrane forming a stable, protein-lined pore that cannot be resealed simply by applying a membrane "patch" or by reducing membrane tension. Intriguingly, studies revealed that mammalian cells have an efficient mechanism to repair their plasma membrane after permeabilization with pore-forming proteins, and this process also requires the presence of extracellular Ca^{2+} [12]. This finding raised the question of whether transmembrane pore removal from the cell surface was also a rapid process, as observed with mechanical wounds[5]. Surprisingly, our recent studies revealed that the resealing of cells permeabilized with pore-forming toxins has very similar properties to the repair of mechanical wounds: the process requires extracellular Ca^{2+}, and is completed within ~30 sec. Investigating this process in more detail, we recently learned that in addition to Ca^{2+}-regulated exocytosis of lysosomes, plasma membrane repair involves a rapid form of endocytosis, which is triggered by release of the lysosomal enzyme acid sphingomyelinase (ASM) and is essential not only for the removal of transmembrane pores, but also for the repair of mechanical wounds[16].

To determine the kinetics of cell resealing after permeabilization with pore-forming proteins, in our laboratory we adapted a live imaging methodology that had been used previously to assess resealing of laser-injured isolated muscle fibers[17]. This assay relies on properties of the lipophilic dye FM1-43, which stably intercalates into the outer leaflet of lipid bilayers increasing in fluorescence intensity. When the

plasma membrane bilayer is disrupted extracellular dye gains access to intracellular membranes, providing a sensitive assay to detect plasma membrane injury and repair[18,16,19,20]. To adapt this assay for the assessment of cell resealing after permeabilization with pore-forming proteins, we pre-incubated cells at 4 °C with the bacterial toxin streptolysin O (SLO), which binds to membrane cholesterol[21]. Synchronous cell permeabilization can then be easily achieved by moving the cells from ice to warm medium in a heated microscope stage, which activates the oligomerization and change in conformation that leads to transmembrane pore formation. An advantage of this approach, over the previously published assays using laser wounding, is that a larger number of cells can be analyzed simultaneously in a microscopic field, providing better sampling of the cell population. Given the mechanistic similarities between the cell resealing process seen after mechanical injury and permeabilization with pore-forming toxins, the assay we describe here provides a very versatile and powerful method for dissecting factors involved in the fundamental process of plasma membrane repair. As an example, we show that it is possible to use this assay to identify Ca^{2+} dependent and independent steps of the repair process.

Protocol

1. Transcriptional Silencing of ASM

1. Seed 1.5 x 10^5 HeLa cells in 2 ml of DMEM growth media (DMEM high glucose with 10% fetal bovine serum (FBS), 2 mM L-glutamine, 1% Penn-Strep) on 35 mm glass bottom dishes (MatTek) and incubate overnight at 37 °C in a 5% CO_2 incubator.
2. On the following day, aspirate off the growth media and replace it with 2 ml DMEM reduced serum medium (DMEM with 4% FBS), at least 1 hr before adding the siRNA transfection mixture.
3. Prepare 4 tubes for the siRNA oligo transfection mixture. In tubes A and C, add 250 µl Optimem reduced serum and 4 µl Lipofectamine RNAiMax, per 35 mm dish to be transfected. In tube B, add 250 µl of Optimem reduced serum and 8 µl (160 pmoles) of control medium GC content oligo (Control siRNA), per 35 mm dish to be transfected. In tube D, add 250 µl of Optimem reduced serum and 8 µl (160 pmoles) of SMPD1 oligo (siASM), per 35 mm dish to be transfected. Incubate the tubes at room temperature for 5 min.
4. Combine tubes A and B to form the transfection complex for Control siRNA, and tubes C and D for the ASM siRNA . Incubate the reactions at room temperature for 20 min.
5. Add the Control siRNA and ASM siRNA transfection reaction mixtures slowly, dropwise, into the respective 35-mm glass bottom dishes and incubate at 37 °C/5% CO_2. At 24 hr post-transfection, gently aspirate off media and replace with fresh DMEM growth media. For efficient ASM knockdown, the dishes should be further incubated at 37 °C/5% CO_2 for about 31 hr (total 55 hr) before live imaging.

2. Preparation of Reagents for Live Microscopy

1. Prepare a solution of recombinant pore-forming toxin Streptolysin O (SLO) at a concentration of 100 ng/µl in cold 1x PBS without Ca^{2+} and Mg^{2+}. The SLO used in these assays is a constitutively active cysteine mutant that does not require reducing agents for activity, kindly provided by Dr. Rod Tweten, University of Oklahoma. The toxin was expressed in *E. coli* BL21 DE3 and purified under native conditions, as described previously[16].
2. Prepare the FM1-43 stock solution: Resuspend FM1-43 lyophilized powder in DMSO to create a 25 mM solution.
3. Prepare Solution A: Dilute the FM1-43 stock solution in cold DMEM with Ca^{2+} to a final concentration of 4 µM (1.5 ml are needed per MatTek dish) and store on ice until needed.
4. Prepare Solution B: Dilute the FM1-43 stock solution in cold DMEM without Ca^{2+} and 10 mM EGTA (Ca^{2+}-free DMEM) to a final concentration of 4 µM (1.5 ml needed per MatTek dish) and store on ice until needed.
5. Pre-warm (37 °C) 1 ml aliquots of Solution A and Solution B in Eppendorf tubes.
6. Keep on ice solutions of DMEM with Ca^{2+}, and Ca^{2+}-free DMEM.

3. Live Cell Imaging of FM1-43 Influx into SLO Treated and Untreated Cells

1. Fill a medium size shallow metal container with crushed ice, invert it into a large glass container with ice, and add additional ice leaving only the bottom surface of the metal container exposed. Place a wet paper towel on the exposed metal bottom to allow for even thermal transfer.
2. Take one Control siRNA-treated MatTek dish (**Sample 1**) and place it on the cold wet paper towel. Gently aspirate off all media and wash 3x with cold Ca^{2+}-free DMEM. After the last wash, aspirate off all media in the dish.
3. To image cell-associated FM1-43 in cells with no SLO wounding (**Sample 1**) in the presence of Ca^{2+}, add 180 µl of cold Solution B to the center glass coverslip of the 35-mm glass bottom dish and incubate for 5 min on ice (**Table 1**).
4. Place MatTek dish on the stage of a confocal microscope heated to 37 °C and equipped with an environmental chamber (which maintains temperature, humidity and CO_2 levels). Find the field of cells that will be imaged looking through a 40X NA 1.3 objective (Nikon). If available, turn on PerfectFocus or a similar device to correct for thermal drift.
5. Add 1 ml of prewarmed Solution A gently to the side of the 35-mm dish and replace cover of environmental chamber (**Table 1**).
6. Acquire images for 4 min at 1 frame every 3 sec using appropriate imaging software (Volocity in the UltraView Vox Perkin Elmer spinning disk confocal microscopy system). Excitation of FM1-43 is accomplished with a 488 nm laser line using a dichroic filter with a 488 nm band pass, and emission discrimination is achieved through use of a 527(W55) emission filter. Laser power levels and camera sensitivity are set to achieve image exposures of 100 msec.
7. Repeat steps 3.2 to 3.6 to detect FM1-43 in Control siRNA-treated cells with no SLO wounding (**Sample 2**) in the absence of Ca^{2+}, except that at step 3.5 Solution B should be added (**Table 1**).
8. To measure FM1-43 influx into Control siRNA-treated cells wounded with SLO either in the presence (**Sample 3**) or absence of Ca^{2+} (**Sample 4**), add 180 µl of cold Solution B containing SLO to the center glass coverslip of the 35-mm glass bottom dish and incubate for 5 min on ice as in step 3.3. Repeat steps 3.2 through 3.6; adjust adding either Solution A or Solution B at step 3.5 (**Table 1**).
9. To determine the role of ASM in plasma membrane repair, repeat steps 3.2-3.6 using ASM siRNA-treated cells for all conditions (**Samples 5-8**) (**Table 1**).

10. To determine the role of extracellular recombinant sphingomyelinase (SM) on the kinetics of plasma membrane repair (reflected by the inhibition in FM1-43 influx) (**Samples 9-10**), SM is added (0-50 µU) to either Solution A or Solution B in step 3.5 and then added to cells during live cell imaging in a total volume of 1 ml (**Table 1**).

4. Quantification of FM1-43 Influx Into Cells

1. After movies have been acquired, measure the intracellular fluorescence intensity of FM1-43 using image analysis software (Volocity Suite, PerkinElmer). Draw a region of interest in the cytosolic region of each cell in the field and apply the software tools to determine the mean FM1-43 fluorescence intensity throughout all frames of the video.
2. To adjust for variations in the initial FM1-43 staining, the data for each video is expressed as fold increase in fluorescence intensity over time, and plotted for each different condition. The fold increase in fluorescence of each individual timepoint per cell is calculated as F_T/F_0, where F_T is the mean fluorescence at the specific timepoint, and F_0 is the mean fluorescence at t = 0 (**Figures 1-2**).

Representative Results

Low concentrations of bacterial sphingomyelinase (SM) rescue plasma membrane repair in cells depleted in lysosomal acid sphingomyelinase.

Using the FM1-43 imaging assay, we previously showed that cells deficient for the lysosomal enzyme ASM and exposed to SLO wounding in the presence of Ca^{2+} have a plasma membrane defect is rescued by extracellular addition of the recombinant human enzyme[19]. Since the human lysosomal ASM has a low pH optimum, we investigated whether resealing could also be restored adding SM purified from *Bacillus cereus* (Sigma), which is fully active at neutral pH. As previously shown, cells treated with Control siRNA or ASM siRNA oligos and exposed to SLO in the absence of Ca^{2+} (conditions not permissive for repair) were equally permeabilized, showing that ASM depletion does not interfere with sensitivity to the toxin (**Figure 1A**). Interestingly, a full rescue of the ability of ASM-deficient cells to reseal after exposure to SLO was observed with low concentrations of SM, 5 and 7.5 µU/ml (**Figure 1B**). As the enzyme concentration added to the medium increased, there was a gradual loss in the rescue phenotype - cells exposed to 10 µU/ml only partially blocked the influx of FM1-43 after exposure to SLO, and cells exposed to 50 µU/ml showed a strong dye influx pattern, reflecting a full resealing defect similar to that observed in ASM-depleted cells (**Figures 1B** and **1C**). This result suggests that endocytic removal of SLO pores is tightly regulated by the ceramide levels generated at the plasma membrane by SM - above a certain level the process does not occur normally, and cells cannot remove the lesions.

Sphingomyelinase addition bypasses the requirement for Ca^{2+} in plasma membrane repair.

Remarkably, addition of bacterial SM to cells permeabilized by SLO in the absence of Ca^{2+} (normally a condition that does not allow cell resealing) also rescued plasma membrane repair. As seen in cells exposed to the pore-forming toxin in the presence of Ca^{2+} (**Figures 1B** and **1C**), only low concentrations of SM were effective in blocking influx of FM1-43 (**Figure 2A** and **2B**). These results indicate that sphingomyelinase functions downstream of the Ca^{2+}-dependent step of plasma membrane repair. This finding is fully consistent with our previously proposed model, which postulates that Ca^{2+} flowing through transmembrane pores triggers exocytosis of lysosomes and ASM release, which cleaves sphingomyelin on the outer leaflet of the plasma membrane, generating ceramide and promoting pore removal by endocytosis[22,19]. The fact that addition of purified SM bypasses the need for Ca^{2+} strongly reinforces the view that under physiological conditions Ca^{2+}-regulated exocytosis of lysosomes is the source of the sphingomyelinase activity required to promote endocytosis.

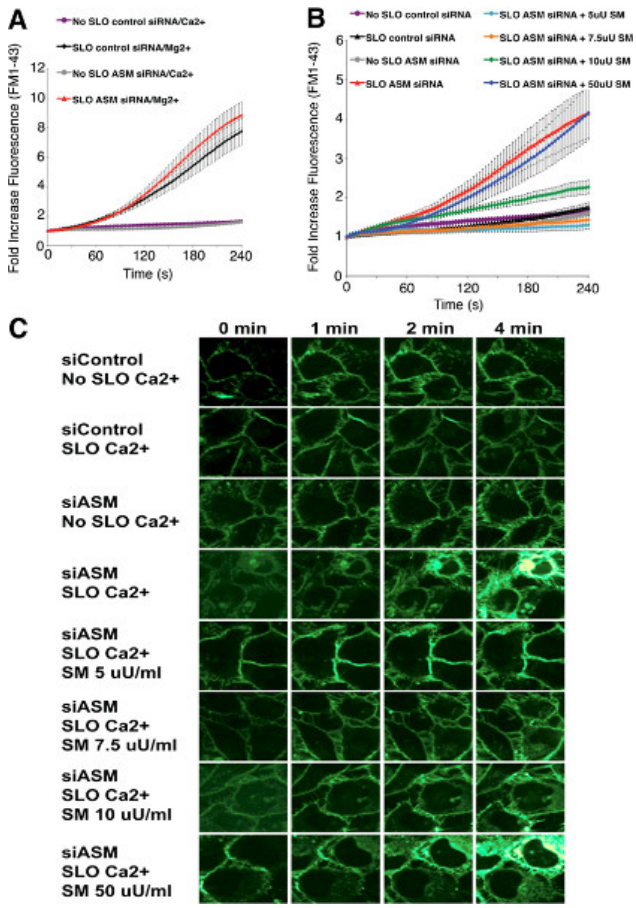

Figure 1. *Bacillus cereus sphingomyelinase* (SM) can complement the plasma membrane repair defect of cells silenced for expression of acid sphingomyelinase (ASM) wounded by the pore-forming toxin streptolysin O (SLO). HeLa cells treated with Control siRNA or ASM siRNA oligos were wounded in the absence or presence of Ca^{2+} and influx of the lipophilic dye FM1-43 was imaged at 1 frame/3 sec for 4 min. FM1-43 intracellular fluorescence was quantified using Volocity software and expressed as fold increase in fluorescence intensity over time. **(A)** In the absence of Ca^{2+}, both Control siRNA and ASM siRNA-treated cells were permeabilized by SLO. 18-27 cells were analyzed in each condition; error bars correspond to the mean +/- SEM. **(B)** In the presence of Ca^{2+}, cells treated with Control siRNA were able to reseal their plasma membrane and stop dye influx, while cells treated with ASM siRNA failed to reseal. Additionally in the presence of Ca^{2+}, exogenous addition of low doses of sphingomyelinase complements the plasma membrane defect of ASM siRNA-treated cells. 18-62 cells were analyzed in each condition; error bars correspond to the mean +/- SEM. **(C)** Selected time frames of the movie analyzed in **B**. Bars, 9 µm. Click here to view larger figure.

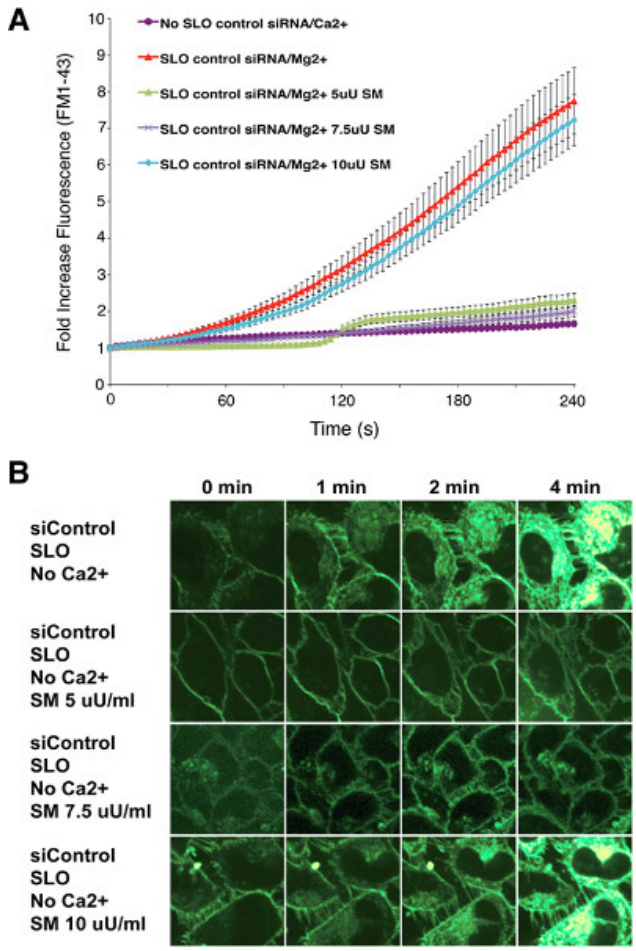

Figure 2. Sphingomyelinase addition bypasses the requirement for Ca^{2+} in plasma membrane repair. HeLa cells treated with Control siRNA were wounded with SLO in the absence of Ca^{2+} and influx of the lipophilic dye FM1-43 was imaged at 1 frame/3 sec for 4 min. FM1-43 intracellular fluorescence was quantified using Volocity software and expressed as fold increase in fluorescence intensity over time. **(A)** The lack of plasma membrane resealing normally seen in cells injured with SLO in the absence of Ca^{2+} is reversed by the exogenous addition of low doses of sphingomyelinase. 18-31 cells were analyzed in each condition; error bars correspond to the mean +/- SEM. **(B)** Selected time frames of the movie analyzed in **A**. Bars, 9 µm. Click here to view larger figure.

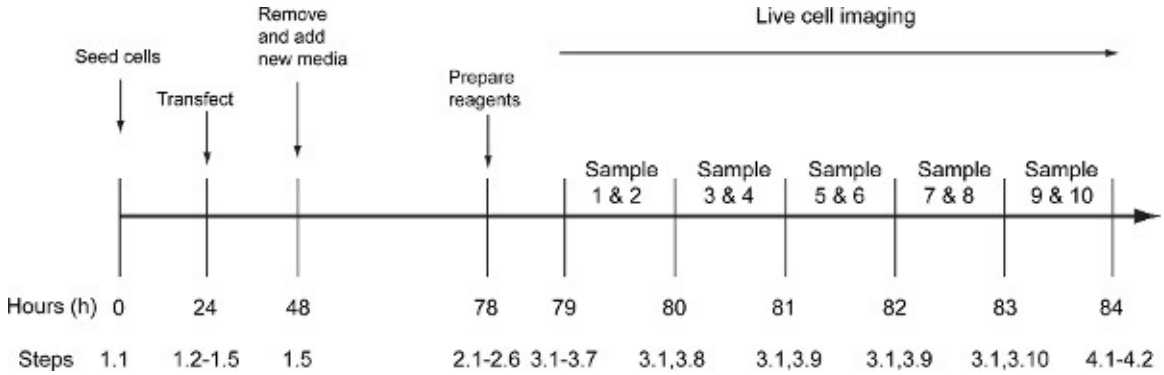

Figure 3. Procedure timeline. Timeline for the experimental steps involved in the procedure. Click here to view larger figure.

Ca2+-condition	Ca2+-free condition	SLO toxin	Warm Solution A	Warm Solution B	Sphingomyelinase	Procedure Step
+	-	-	+	-	-	3.2
-	+	-	-	+	-	3.7
+	-	+	+	-	-	3.8
-	+	+	-	+	-	3.8
+	-	-	+	-	-	3.9
-	+	-	-	+	-	3.9
+	-	+	+	-	-	3.9
-	+	+	-	+	-	3.9
-	+	+	-	+	+	3.10
+	-	+	+	-	+	3.10

Table 1. Composition of solutions used in the experimental procedure. Samples as described in the procedure are listed in rows. Columns denote the presence (+) or absence (-) of the named component (oligo, Ca^{2+} or Ca^{2+}-free medium, SLO, Solution A or B, sphingomyelinase). The experimental steps in which these samples are first used for live cell imaging in the Procedure Section 3 are indicated.

Discussion

Earlier studies on mechanical injury and plasma membrane repair relied on diverse mechanisms of injuring cells, ranging from dropping glass beads, micropipetting, shearing, scratching or scraping. The readout of all these assays was qualitative rather than quantitative, and did not give precise information on the kinetics of the repair mechanism. The ability of cells to reseal their plasma membrane after these forms of injury was measured by the presence or absence of tracers added to the extracellular fluid in the cytoplasm, penetration of membrane impermeable dyes, loss of cytosolic enzymes, ATP levels, or long-term cellular survival. Although several of these assays can be performed quantitatively, one major obstacle in these studies was the difficulty in synchronizing the wounding event, while rapidly assessing the kinetics of resealing at the single cell level.

The development and use of UV-laser injury of muscle fibers followed by detection of the influx of the lipophilic dye FM1-43 was a major advance in these studies[17,20]. Instead of the gross damage inflicted to the whole cell population by scraping or similar mechanical means of injury, these assays introduced a more defined way to wound cells that allowed single cell analysis. However, several problems remained in such assays. The size of laser-induced lesions is large and quite variable depending on laser intensity, and very different in nature than the forms of membrane injury that occur during physiological conditions. Another problem is that only one cell or muscle fiber can be wounded at a time using microscope-associated lasers, reducing the numbers of resealing events that can be followed, and thus the statistical significance of the results. These problems with reproducibility and sampling greatly reduced the usefulness of laser injury as a method to investigate mechanisms of plasma membrane repair.

To address these issues, we developed a new live cell imaging assay to precisely measure the repair kinetics of plasma membrane lesions caused by bacterial pore-forming toxins. This is a form of injury that occurs frequently in nature, since many microbes possess numerous toxins that are capable of permeabilizing the membrane of eukaryotic cells. This assay can be precisely synchronized by pre-incubating the cells with the toxin at low temperatures, and allows a large number of cells in a microscopic field to be analyzed for influx of FM1-43, as the temperature is increased to trigger pore formation.

The precise synchronization of pore-formation achieved with this assay allows reproducible measurements of the plasma membrane repair kinetics, which can be quantitated simultaneously in several individual cells within the microscopic field. One important technical factor in these assays is the quality of the microscope objective lens to be used for imaging. The 40X NA 1.3 (Nikon) objective used in our assays allows for a sufficient sampling of cells in a population without losing image resolution. Switching to a 10X objective would allow a larger sampling of the cell population, but the resolution that is achieved is insufficient for proper quantification of intracellular FM1-43. A critical step for this live cell imaging assay is the use of PerfectFocus or a similar device to correct for thermal drift. Our procedure requires pre-binding of bacterial pore-forming toxin to cells on ice and then shifting the temperature quickly to 37 °C for live cell imaging. This temperature adjustment will cause axial focus fluctuations during the image acquisition period, and must be corrected. PerfectFocus or a similar device will correct this problem allowing live cell imaging of a selected focal plane over extended periods of time, thus allowing precise quantification of the plasma membrane repair kinetics.

A key to the success of this assay is to always titer different concentrations of the pre-forming toxin to determine repairable and non-repairable doses, since this can vary for each batch of toxin used. The activity of many toxins, and of SLO in particular, is temperature sensitive and multiple freeze-thaws cycles are detrimental to its activity. However, titrations performed alongside in each experiment allow the correct toxin dose to be precisely determined in only a few minutes of time-lapse imaging.

This assay relies on the detection of sufficient intracellular FM1-43 fluorescence after plasma membrane injury. This can be limiting under certain conditions. After inserting into membranes SLO forms pores with a diameter of about 30 nm, allowing for robust Ca^{2+} influx and a rapid plasma membrane repair response in eukaryotic cells. However, pore-forming toxins that form smaller lesions, such as aerolysin and lysenin that have pore diameters of about 1-3 nm[23-25] may not be adequate for this assay since they may result in insufficient Ca^{2+} and FM1-43 influx.

Even using a toxin that generates large pores such as SLO, it is important to keep in mind that this imaging assay does not allow for absolute quantification of fluorescence intensity, but rather relative fluorescence. Thus, it is critical that imaging is performed within the intrascene dynamic range of the digital camera. Since the fluorescence intensity is affected by laser power, exposure time, and camera gain, it is important to set these three parameters at the beginning of each experiment, by performing preliminary imaging of cells treated with FM1-43 and SLO in both repair and non-repair conditions (Ca^{2+} or Ca^{2+}-free medium). This allows the choice of image acquisition settings that allow fluorescence detection at time zero (before SLO addition) but do not result in detector saturation (as determined by software readout) at the end of acquisition under non-repair conditions.

Using this assay, we were able to demonstrate that SLO pores are removed from the plasma membrane of mammalian cells in less than 30 sec, demonstrating that this process has a rapid kinetics similar to the repair of mechanical wounds[16]. Subsequent studies showed that the lysosomal enzyme ASM is required for plasma membrane repair, and capable of restoring resealing when added extracellularly to ASM-deficient cells[19]. In the present study, we took advantage of the sensitivity of the FM1-43 influx assay to show, for the first time, that plasma membrane repair can also occur in the absence of extracellular Ca^{2+}. Exposure of wounded cells to recombinant sphingomyelinase was sufficient to promote resealing in cells permeabilized by SLO in Ca^{2+} free medium, a condition normally not permissive for plasma membrane repair. Interestingly, complementation of the plasma membrane repair capacity was not observed after exposure to high concentrations of sphingomyelinase, suggesting that the amount of ceramide generated by this enzyme on the outer leaflet of the plasma membrane is an important determinant of the lesion removal process. This finding demonstrates that Ca^{2+} is necessary to trigger the lysosomal exocytosis step, but is not needed for the sphingomyelinase-induced endocytosis that is responsible for wound internalization.

Disclosures

The authors declare they have no competing financial interests.

Acknowledgements

This work was supported by NIH grants R37 AI34867 and R01 GM064625 to N.W.A. We thank Dr. R. Tweten from the University of Oklahoma for the SLO expression plasmid.

References

1. Heilbrunn, L. In: *The dynamics of living protoplasm.*, Academic Press, (1956).
2. Chambers, R. & Chambers, E. In *Explorations into the nature of the living cell.* Harvard University Press, (1961).
3. Bi, G.Q., Alderton, J.M. & Steinhardt, R.A. Calcium-regulated exocytosis is required for cell membrane resealing. *J. Cell Biol.* **131**, 1747-1758 (1995).
4. Miyake, K. & McNeil, P.L. Vesicle accumulation and exocytosis at sites of plasma membrane disruption. *J. Cell Biol.* **131**, 1737-1745 (1995).
5. Steinhardt, R.A., Guoqiang, B., & Alderton, J.M. Cell membrane resealing by a vesicular mechanism similar to neurotransmitter release. *Science.* **263**, 390-393 (1994).
6. McNeil, P.L., Vogel, S.S., Miyake, K., & Terasaki, M. Patching plasma membrane disruptions with cytoplasmic membrane. *J. Cell Sci.* **113**, 1891-1902 (2000).
7. Togo, T., Alderton, J.M., Bi, G.Q., & Steinhardt, R.A. The mechanism of facilitated cell membrane resealing. *J. Cell Sci.* **112**, 719-731 (1999).
8. Rodriguez, A., Webster, P., Ortego, J., & Andrews, N.W. Lysosomes behave as Ca^{2+}-regulated exocytic vesicles in fibroblasts and epithelial cells. *J. Cell Biol.* **137**, 93-104 (1997).
9. Reddy, A., Caler, E., & Andrews, N. Plasma membrane repair is mediated by Ca^{2+}-regulated exocytosis of lysosomes. *Cell.* **106**, 157-169 (2001).
10. Jaiswal, J.K., Andrews, N.W., & Simon, S.M. Membrane proximal lysosomes are the major vesicles responsible for calcium-dependent exocytosis in nonsecretory cells. *J. Cell Biol.* **159**, 625-635 (2002).
11. Chakrabarti, S., *et al.* Impaired membrane resealing and autoimmune myositis in synaptotagmin VII-deficient mice. *J. Cell Biol.* **162**, 543-549 (2003).
12. Walev, I., *et al.* Delivery of proteins into living cells by reversible membrane permeabilization with streptolysin-O. *Proc. Natl. Acad. Sci. U.S.A.* **98**, 3185-3190 (2001).
13. Iacovache, I., van der Goot, F.G., & Pernot, L. Pore formation: an ancient yet complex form of attack. *Biochim. Biophys. Acta.* **1778**, 1611-1623 (2008).
14. Morgan, B.P. & Campbell, A.K. The recovery of human polymorphonuclear leucocytes from sublytic complement attack is mediated by changes in intracellular free calcium. *Biochem. J.* **231**, 205-208 (1985).
15. Keefe, D., *et al.* Perforin triggers a plasma membrane-repair response that facilitates CTL induction of apoptosis. *Immunity.* **23**, 249-262 (2005).
16. Idone, V., *et al.* Repair of injured plasma membrane by rapid Ca^{2+}-dependent endocytosis. *J. Cell Biol.* **180**, 905-914 (2008).
17. Bansal, D., *et al.* Defective membrane repair in dysferlin-deficient muscular dystrophy. *Nature.* **423**, 168-172 (2003).
18. McNeil, P.L., Miyake, K., & Vogel, S.S. The endomembrane requirement for cell surface repair. *Proc. Natl. Acad. Sci. U.S.A.* **100**, 4592-4597 (2003).
19. Tam, C., *et al.* Exocytosis of acid sphingomyelinase by wounded cells promotes endocytosis and plasma membrane repair. *J. Cell Biol.* **189**, 1027-1038 (2010).
20. Weisleder, N., *et al.* Visualization of MG53-mediated cell membrane repair using *in vivo* and *in vitro* systems. *J. Vis. Exp.* (52), e2717, doi:10.3791/2717 (2011).
21. Tweten, R.K. Cholesterol-dependent cytolysins, a family of versatile pore-forming toxins. *Infect. Immun.* **73**, 6199-6209 (2005).
22. Zha, X., *et al.* Sphingomyelinase treatment induces ATP-independent endocytosis. *J. Cell Biol.* **140**, 39-47 (1998).
23. Buckley, J.T. Crossing three membranes. Channel formation by aerolysin. *FEBS Lett.* **307**, 30-33 (1992).

24. Parker, M.W., *et al.* Structure of the Aeromonas toxin proaerolysin in its water-soluble and membrane-channel states. *Nature*. **367**, 292-295(1994).
25. Yamaji-Hasegawa, A., *et al.* Oligomerization and pore formation of a sphingomyelin-specific toxin, lysenin. *J. Biol. Chem.* **278**, 22762-22770 (2003).

